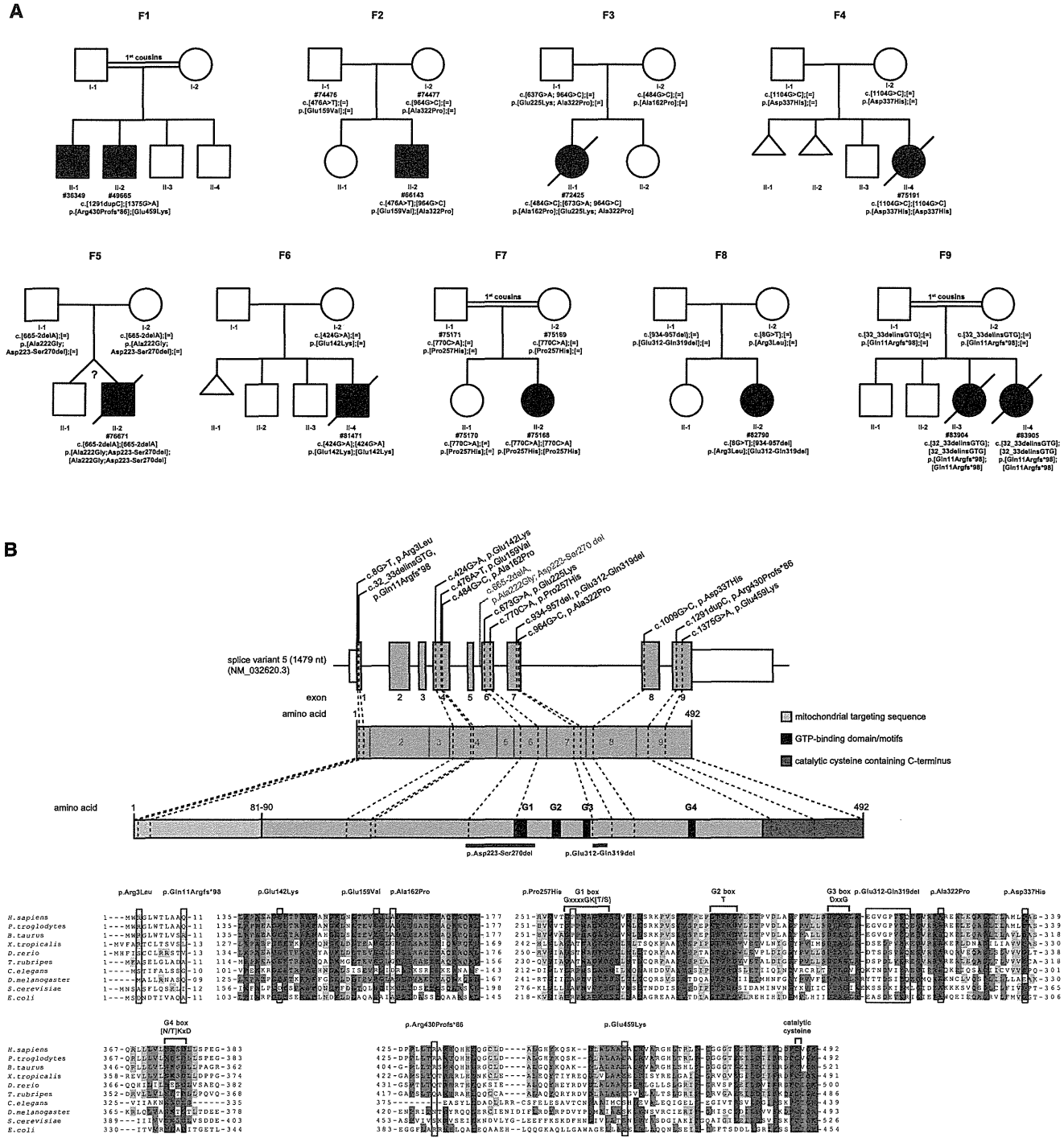

Figure 1. *GTPBP3* Mutation Status and Gene Structure
(A) Pedigrees of nine families with mutations in *GTPBP3*.
(B) Gene structure of *GTPBP3* with known protein domains of the gene product and localization and conservation of amino acid residues affected by mutations. Black and orange text indicate exonic and intronic variants. Intronic regions are not drawn to scale. Coloring in the sequence alignment represents the identity of amino acid residues.

she developed recurrent cough and fever and was admitted to the emergency room with severe fatigue, pallor, and progressive malaise. Blood exams showed leukocytosis, and 2 days later her general condition worsened, showing cyanosis and hyporeactivity. Echocardiography showed severe dilated cardiomyopathy with an ejection fraction of 20% that was unresponsive to therapy. She had severe refractory hyperlactatemia (23.3 mmol/l, reference range 0.5–2.3 mmol/l). Histochemical and spectrophotometric analysis of the muscle biopsy showed a severe complex IV deficiency. She died 10 days after admission from cardiac failure.

Individual #75191 (family F4, Figure 1A), a girl, was born to nonconsanguineous parents after an uneventful pregnancy of 40 weeks. The mother had had two miscarriages at 6 and 8 weeks and had a healthy son aged 16 months. In the first hours after birth, individual #75191 developed mild stridor and dyspnea which rapidly worsened. She fed poorly and became less responsive, and a Kussmaul breathing pattern was seen. She was transferred to a specialist center and was found to be severely hypotonic, moving very little, either spontaneously or after stimulation. She had hyperlactatemia (23 mmol/l), hypoglycemia (18 mg/dl), hyperammonemia (135 μmol/l, control value 11–48 μmol/l), and hyperlactaturia. She progressively developed respiratory insufficiency and bradycardia. Cardiac ultrasound showed apical right ventricular hypertrophy and an open duct of Botalli with minor shunting. Fractional shortening was 28% (mildly decreased). Cerebral ultrasound showed a minimal grade I bleeding, and the cerebral matter appeared mildly hyperechogenic. She died of asystolia at day 1. A muscle biopsy performed immediately after death showed decreased activities of RC complexes I and IV.

Individual #76671 (family F5, Figure 1A) was the second boy of nonconsanguineous parents. The infant was born at 41 weeks of gestation from a twin pregnancy. Generalized hypotonia and difficulty in suction was noted since birth and he rapidly developed failure to thrive. He acquired head control at the age of 7 months but parents reported normal cognitive skills. At the age of 9 months he was admitted to the intensive care unit for acute aspiration pneumonia that required intubation. Laboratory test revealed a metabolic acidosis with hyperlactatemia (5.2 mmol/l) and brain MRI showed bilateral thalamic T2-weighted hyperintense abnormalities with low diffusion. Analysis of a muscle biopsy revaled a clear reduction in histochemical cytochrome *c* oxidase activity and decreased complex I and IV enzyme activities. The cardiological examination disclosed hypertrophic cardiomyopathy and a Wolff-Parkinson-White pre-excitation syndrome (MIM 194200). The baby died after 15 days of hospitalization with clinical signs of heart failure.

Individual #81471 (family F6, Figure 1A) was a boy born to nonconsanguineous Romanian parents at 34 weeks gestation (birth weight 2.18 kg). His mother had premature and prolonged (85 hr) rupture of membranes before delivery, and the baby was treated with i.v. antibiotics before being discharged home on day 7. He was readmitted to hospital on day 25 with weight loss (2.23 kg). He was hypothermic and jaundiced and initial blood analysis showed profound metabolic acidosis. He was treated with i.v. antibiotics for presumed sepsis. The acidosis did not resolve, and serum lactate was elevated (11.0 mmol/l). ECG was abnormal and echocardiography showed concentric left ventricular hypertrophy. CSF lactate was 12.4 mmol/l (normal range 0.9–2.4 mmol/l) prompting bicarbonate treatment. Brain MRI showed abnormal diffusion of the subthalamic nuclei extending down to the brain stem. There was abnormal T2 signal in the midbrain and basal ganglia bilaterally. On examination he was thin but not dysmorphic. He was mildly jaundiced and had puffy feet. There was little spontaneous movement but normal muscle bulk and he was distinctly hypotonic. Feeding through a nasogastric tube was established but he did not become responsive despite high caloric intake. He developed recurrent apnea and died aged 5 weeks. Biochemical analysis performed in muscle revealed a significant decrease of RC complexes I and IV.

Individual #75168 (family F7, Figure 1A) is the second girl of first-cousin parents from India. She was first seen at the age of 2 years with development delay. She was able to walk but she couldn't speak. She received occupational and speech therapy. During a febrile illness when she was 3 years old, she had an acute metabolic failure with hyperlactatemia and hyperlactatorachia. She recovered but had epileptic seizures and more severe intellectual disability. Brain MRI showed pronounced bilateral hyperintensities affecting the whole thalamus and extending to the mesencephalon. Hyperlactatemia (>10 mmol/l) and hyperlactatorachia (6 mmol/l) were noticed. RC activity in muscle was normal as well as PDH complex tested by immunoblot. The girl was treated with qa carnitine 3 × 350 mg/day, CoQ_{10} 3 × 50 mg/day, vitamins B1 3 × 50 mg/day and B6 3 × 50 mg/day, and bicarbonate 4 × 1 g. Epilepsy was in good control with levetiracetame 40 mg/kg/day and a high-fat diet. The girl is in a special school for children with developmental delay. Her general condition is good. She is always in a good temper. Development is delayed about 1.5 years. She has continual hyperlactatemia (8–10 mmol/l).

Individual #82790 (family F8, Figure 1A) is a girl born at 40 weeks of gestation with normal birth weight to nonconsanguineous Japanese parents. At the age of 1 year, she developed frequent epileptic seizures, and she was medicated with phenobarbital. Severe developmental delay was noted and at the age of 15 months she was admitted to children's hospital. Her weight gain (9.25 kg, −0.06 SD) is within the normal range, but she developed severe muscle hypotonia. There is no cardiac involvement by ECG and echocardiogram. Hyperlactatemia was noted (5.72–6.49 mmol/l) whereas metabolic profiling of amino acids, urinary organic acids, and acylcarnitine was normal. RC analysis in muscle showed a significant decrease in complexes I and IV activities. Brain MRI showed bilateral hyperintensities in the putamen and weakly also in the anterior thalamus. A lactate peak was detected on $[H^+]$-MR spectroscopy. She is now 2 years of age and still presents with a severe global developmental delay.

Individual #83904 (family F9, Figure 1A) was the second child of consanguineous, healthy parents of Turkish origin. She was born at 39 weeks of gestational age (birth weight 2,740 g, length 49 cm, head circumference 32 cm). Shortly after birth, she presented with Wolff-Parkinson-White syndrome. Cardiac ultrasound was normal. Treatment was started with amiodarone and she

Table 1. Genetic and Clinical Findings in Individuals with *GTPBP3* Mutations

		GTPBP3 Mutations	OXPHOS Activities in Skeletal Muscle				Clinical Features				
ID	Sex	cDNA (NM_032620.3) and Protein (NP_116009.2)	RCC	% of Lower Control Range	Absolute Values	Reference Range	AO	Course	HCM	Histochemical COX Defect	Other Features
#49665[a,b]	male	c.[1291dupC; 1375G>A], p.[Pro430Argfs*86; Glu459Lys]	I	15%	0.025	0.17–0.56	10 years	alive 14 years	yes	ND	consanguineous parents (1st cousins), mild intellectual disability, fatigability, limited vision, lactic acidosis
			II	ND	ND	ND					
			II+III	normal	0.201	0.08–0.48					
			IV	24%	0.267	1.1–5.0					
#36349[b]	male	c.[1291dupC; 1375G>A], p.[Pro430Argfs*86; Glu459Lys]	I	no data	no data	no data	no data	alive 17 years	no data	no data	sibling of #49665 with similar clinical symptoms
			II								
			II+III								
			IV								
#66143[a]	male	c.[476A>T; 964G>C], p.[Glu159Val; Ala322Pro]	I	7%	0.01	0.19–0.48	2 years	alive 5 y ears	yes	ND	unrelated parents, sudden respiratory failure, lactic acidosis
			II	normal	0.10	0.07–0.12					
			II+III	normal	0.12	0.09–0.22					
			IV	28%	0.12	0.44–0.92					
#72425[a]	female	c.[484G>C; 673G>A; 964G>C], p.[Ala162Pro; Glu225Lys; Ala322Pro]	I	14%	0.015	0.11–0.30	3.5 months	died 8 months	DCM	yes	unrelated parents, cyanosis, hyporeactivity, DCM with residual ejection fraction of 20%, lactic acidosis
			II	normal	0.21	0.12–0.25					
			II+III	normal	0.06	0.006–0.14					
			IV	45%	0.76	1.7–4.0					
#75191[a]	female	c.[1009G>C; 1009G>C], p.[Asp337His; Asp337His]	I	31%	0.03	0.10–0.25	birth	died 1 day	yes	yes	unrelated parents, Kussmaul breathing, stridor, hypotonic, hyporeactivity, RVH, lactid acidosis
			II	normal	0.16	0.14–0.25					
			II+III	normal	0.12	0.13–0.25					
			IV	15%	0.09	0.60–1.48					
#76671	male	c.[665–2delA; 665–2delA], p.[Ala222Gly; Asp223_Ser270del; Ala222Gly; Asp223_Ser270del]	I	45%	0.05	0.11–0.30	birth	died 10 months	yes	yes	unrelated parents, hypotonia from birth, RVH, WPW, lactic acidosis
			II	normal	0.16	0.12–0.25					
			II+III	ND	ND	0.06–0.14					
			IV	17%	0.29	1.7–4.0					
#81471[a]	male	c.[424G>A; 424G>A], p.[Glu142Lys; Glu142Lys]	I	12%	0.012	0.104 ± 0.036	4 weeks	died 5 weeks	yes	yes	consanguineous parents, two healthy siblings, one miscarriage, FTT, poor weight gain and feeding, concentric LVH, lactic acidosis
			II	normal	0.098	0.145 ± 0.047					
			II+III	normal	0.850	0.544 ± 0.345					
			IV	17%	0.127	1.124 ± 0.511					

(*Continued on next page*)

Table 1. *Continued*

		GTPBP3 Mutations	OXPHOS Activities in Skeletal Muscle				Clinical Features				
ID	Sex	cDNA (NM_032620.3) and Protein (NP_116009.2)	RCC	% of Lower Control Range	Absolute Values	Reference Range	AO	Course	HCM	Histochemical COX Defect	Other Features
#75168[a]	female	c.[770C>A; 770C>A], p.[Pro257His; Pro257His]	I	normal	no data	no data	2 years	alive 5 years	no	ND	consanguineous parents (1st cousins), developmental delay, epileptic seizures, intellectual disability, MRI hyperintense lesions of basal ganglia typical to Leigh syndrome, lactic acidosis
			II	normal							
			II+III	normal							
			IV	normal							
#82790[a]	female	c.[8G>T; 934_957del], p.[Arg3Leu; Gly312_Val319del]	I	36%	0.107	0.301 ± 0.05	1 year	alive 2 years	no	ND	unrelated parents, seizures, severe hypotonia, developmental delay, lactic acidosis
			II	normal	0.424	0.272 ± 0.05					
			II+III	normal	0.21	0.25 ± 0.093					
			IV	21%	0.008	0.035 ± 0.011					
#83904[a,c]	female	c.[32_33delinsGTG; 32_33delinsGTG], p.[Gln11Argfs*98; Gln11Argfs*98]	I	64%	4.2	6.5–17	1 week	died 9 months	yes	ND	consanguineous parents (1st cousins), lactic acidosis, WPW
			II	normal	16.1	13.6–45.7					
			II+III	normal	5.8	4.3–13.2					
			IV	25%	9.9	74–294					
#83905[a,c]	female	c.[32_33delinsGTG; 32_33delinsGTG], p.[Gln11Argfs*98; Gln11Argfs*98]	I	no data	no data	no data	birth	died 10 days	yes	ND	consanguineous parents (1st cousins), lactic acidosis, WPW
			II								
			II+III								
			IV								
#66654[a]	female	c.[673G>A; 964G>A]; [=] p.[Glu255Lys; Ala322Pro]; [=]	I	64%	0.09	0.14–0.35	1.5 months	alive	no	ND	intrauterine growth retardation, lactic acidosis, leukodystrophy, generalized hypotonia
			II	normal	0.19	0.18–0.41					
			II+III	90%	0.27	0.30–0.67					
			IV	normal	1.42	0.42–1.26					

Abbreviations are as follows: AO, age of onset; HCM, hypertrophic cardiomyopathy; DCM, dilated cardiomyopathy; FTT, failure to thrive; LVH/RVH, left/right ventricular hypertrophy; ND, not determined; WPW, Wolff-Parkinson-White syndrome.
Mitochondrial respiratory chain complexes (RCC) in muscle: I, NADH:CoQ-oxidoreductase; II, succinate:CoQ-oxidoreductase; II+III, succinate:cytochrome c reductase; IV, cytochrome c oxidase (COX).
Enzyme activities were determined in muscle biopsies and normalized to citrate synthase (CS). Absolute values and reference ranges are given in [mU / mU CS].
[a]Investigated by exome sequencing.
[b,c]These individuals are siblings.

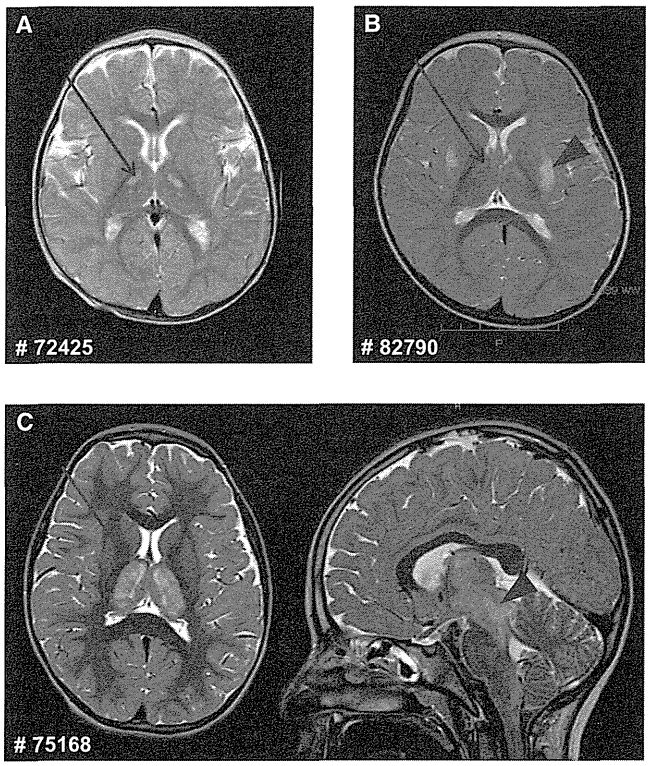

Figure 2. Brain MRI of Affected Individuals #72425, #82790, and #75168

(A) MRI of individual #72425 shows small T2 hyperintensities in the anterior thalamus bilaterally (arrow).

(B) In individual #82790, T2-weighted MRI shows bilateral hyperintensities in the putamen (arrowhead) and weakly also in the anterior thalamus (arrow).

(C) T2-weighted MRI of individual #75168 shows pronounced bilateral hyperintensities affecting the whole thalamus (arrow, axial view at the left) and extending to the mesencephalon (arrowhead, sagittal view at the right).

remained stable, without cardiac symptoms or arrhythmia. At 7 months of age, she had cardiogenic shock and metabolic acidosis. Heart ultrasound detected dilated cardiomyopathy and decreased contractility (ejection fraction 35%). She presented hyperlactatemia (20 mmol/l), hyperalaninemia (1,175 μmol/l; normal range, 190–450 μmol/l), and an increased lactate-to-pyruvate ratio (47; normal range, 10–20). Her disorder progressed despite intensive medication for heart failure. She died at the age of 9 months of cardiac insufficiency with arrhythmia.

Her younger sister, individual #83905 (family F9, Figure 1A), had a very similar clinical picture. She died at 6 months of age of cardiac insufficiency unresponsive to resuscitation procedures.

Genetic, biochemical, and clinical findings are summarized in Table 1. Pedigrees of the families we studied are shown in Figure 1A. The location of the identified mutations within the gene and the conservation of the affected amino acid (aa) residues are shown in Figure 1B. Individual #49665 (F1: II-2) was found to carry a frame shift and one missense variant. The next generation sequencing (NGS) data demonstrated a compound heterozygous status of the two variants (Figure S1 available online). Individual #76671 (F5: II-2) was homozygous for an intronic single base pair deletion, c.665−2delA, which is predicted to cause the loss of a splice acceptor site. Analysis of cDNA from fibroblasts revealed a shorter transcript, and sequencing found that in more than 95% of transcripts, the downstream acceptor of exon 7 was used for splicing, resulting in the skipping of exon 6 including the conserved G1-box guanine nucleotide-binding signature motif (Figure S2). Individual #82790 (F8: II-2) was found to be compound heterozygous for a missense mutation c.8G>T (p.Arg3Leu) and a 24 bp deletion c.934_957del (p.Gly312_Val319del). The 24 bp deletion is predicted to cause the deletion of 8 amino acids containing conserved residues. The p.Arg3Leu substitution at the very N terminus of the protein is scored as a predicted polymorphism but causes a loss of a positively charged residue, which is predicted to interfere with mitochondrial targeting (Predotar, PsortII). The two missense variants found in individual #66654, c.[673G>A; 964G>C], p.[Glu225Lys; Ala322Pro], were identical to the variants found on the paternal allele of individual #72425 (F3: II-1). Analysis of parental DNA revealed that both variants were also located on the same allele in individual #66654, meaning that only one allele is affected. Because of this observation, combined with the absence of a heart phenotype and because this individual is the only one exhibiting an isolated complex I defect, we consider the mutations found in *GTPBP3* not to be causative in subject #66654.

In summary, the identification of 13 different alleles in 11 individuals with suspected mitochondrial disease from 9 families provides strong evidence for the pathological role of mutant *GTPBP3* in the investigated families. It links *GTPBP3* mutations to combined respiratory chain complex deficiency (9/11), cardiomyopathy (9/11), lactic acidosis (11/11), and encephalopathy (4/11).

Brain MRI was performed in three individuals (Figure 2). It showed bilateral T2 hyperintensities in the thalamus, ranging from weak (#82790) or small (#72425) changes in the anterior thalamus to very pronounced hyperintensities affecting the whole thalamus in individual #75168. In addition, T2 hyperintensities affected the putamen bilaterally in individual #82790 and extended markedly to the mesencephalon in individual #75168. Taken together, the MRI involvement of basal ganglia and brainstem resembles the (MRI) findings in Leigh syndrome (which is, however, an ill-defined entity).

Skin fibroblast cell lines were available from seven individuals for functional studies. We first analyzed the cellular oxygen consumption rate (OCR[13]) by microscale respirometry with the XF96 extracellular flux analyzer (Seahorse Bioscience). When cells of individuals from families F1 to F5 were cultured in glucose-containing medium, only cell lines from individuals #75191 (F4: II-4) and #76671 (F5: II-2) showed a decreased OCR (of 59% and 58%, respectively) indicating defective oxidative phosphorylation

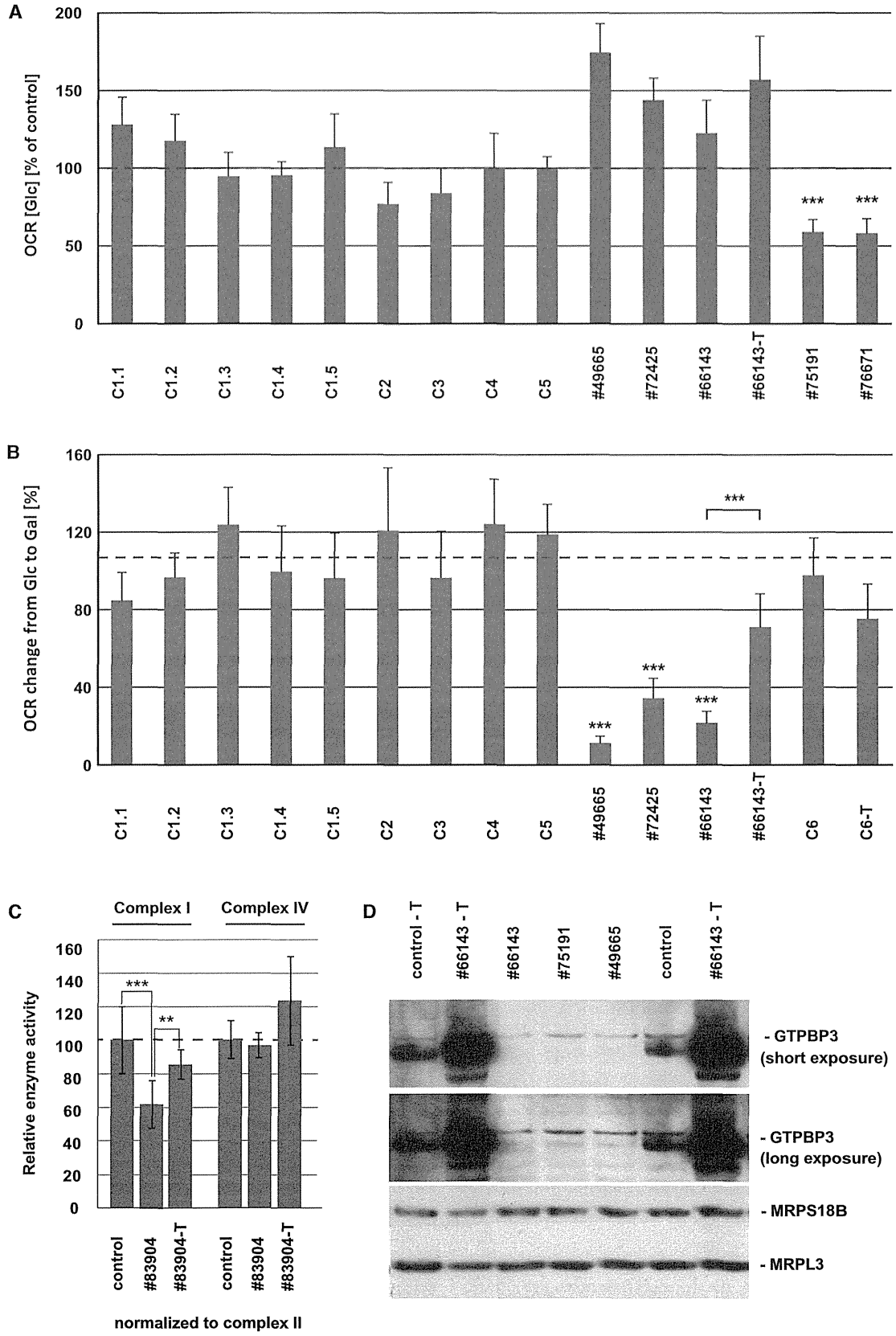

Figure 3. Analysis of Respiration Defects and GTPBP3 Protein Levels in Fibroblast Cell Lines
(A) Oxygen consumption rate (OCR) of fibroblast cell lines from five affected individuals and five control subjects cultured in high-glucose (Glc) medium. Each analysis was performed in more than 15 replicates. Control one (C1) was measured five time at different passage numbers (C1.1–1.5, NHDFneo, Lonza). OCR was expressed as percentage relative to the average of all controls. Cells from

(legend continued on next page)

(Figure 3A). When cells were cultured with galactose as the primary carbon source, rather than glucose, cells are forced to rely on oxidative phosphorylation rather than glycolysis in order to meet the energy demand.[14,15] Accordingly, in control cells an increase in OCR of approximately 2-fold was observed when galactose was substituted as the primary carbon source. This increase in OCR was impaired in fibroblasts from affected individuals #49665 (F1: II-2), #66143 (F2: II-2), and #72425 (F3: II-1), which showed OCR increases of only 11%, 35%, and 22%, respectively (Figure 3B). In order to confirm that defects in GTPBP3 are the cause of this defect, we transduced three cell lines with a wild-type copy of *GTPBP3* cDNA (RefSeq NM_32620.3) by using a lentiviral vector (pLenti 6.3/V5 TOPO, Life Technologies) as previously described.[16,17] Fibroblasts from individuals #49665 and #66143 were used for the rescue experiment, with fibroblasts from #66654 (subject with only one affected allele) being included as a control (C6). Unfortunately, we were unable to recover any viable cells from subject #49665 after the transduction procedure. Although the transduction had no noticeable effect on the control cell line (C6-T), transduced fibroblasts from #66143 (#66143-T) displayed a significant improvement of OCR in galactose-containing medium (Figure 3B). Furthermore, we detected an isolated respiratory chain complex (RCC) I deficiency in a fibroblast cell line from family 9. Cotransfection of individual #83904 fibroblasts with two putative *GTPBP3* isoforms amplified by RT-PCR, RefSeq NM_32620.3 and NM_0128855.2 (missing 63 base pairs of exon 8), significantly improved enzyme activities of RCC I (pIRES2-EGFP, Clontech) (Figure 3C). Analysis of the protein levels of GTPBP3 in five fibroblast cell lines demonstrated reduced or undetectable amounts in individuals #49665, #75191, #66143, #83904, and #83905, although they showed a clear increase after transduction or transfection (Figures S4 and 3D). In conclusion, our data demonstrate a causal role for *GTPBP3* mutations in the oxidative metabolism deficiency in these individuals.

Given that homologs of GTPBP3 in other systems have been implicated in protein synthesis, we next concentrated on the analysis of GTPBP3 in mitochondrial translation. The synthesis of mtDNA-encoded polypeptides, investigated by pulse-labeling of mitochondrial translation products via [^{35}S]methionine in fibroblasts of affected individuals (for methods see Haack et al.[18]) was severely and uniformly decreased to 20%–30% of control levels in individuals #49665, #66143, and #75191 (Figures 4A and 4B). There was no detectable defect in fibroblasts from individual #72425, which might be explained by the relatively low conservation of the mutated residue in this individual (Figure 1B). In order to exclude possible defects of mitochondrial transcription or precursor RNA processing, we analyzed all mitochondrially encoded rRNAs and mRNAs in fibroblasts of individuals #49665, #66143, #72425, and #75191 by RNA blotting and by RNA-seq in fibroblasts of individual #49665. We found no differences in the expression levels of the mt-RNAs between case and control subjects. On average, the mt-RNA expression levels were only 6% lower in individual #49665 as compared to control individuals (data not shown). We did not observe any appreciable reduction in steady-state levels of mature RNAs, nor was there any accumulation of precursor RNAs (Figure S3A). Next, we analyzed the steady-state levels of mt-tRNAs, including those five species for which the τm^5 U modification has been reported in mammals (Gln, Glu, Lys, Leu^{UUR}, and Trp).[4] We again observed no appreciable changes in their steady-state levels (Figure S3B). In order to further corroborate a direct role of GTPBP3 in mitochondrial translation, we downregulated its expression via RNA interference in HeLa cells (Figure 4C). Reduction of GTPBP3 protein levels upon RNAi treatment of HeLa cells was comparable to the reduction of its level in *GTPBP3* mutant fibroblasts (Figure 4D). Downregulation of *GTPBP3* expression resulted in a general mitochondrial translation defect, similarly to the reduction observed in subject fibroblasts (Figure 4D). In conclusion, the reduced translation efficiency observed in three out of four *GTPBP3* mutant cell lines, as well as in human cells treated with *GTPBP3* RNAi, confirmed an important function for GTPBP3 in efficient mitochondrial protein synthesis.

In order to test the consequences of this reduced translation rate upon the protein levels of OXPHOS complexes in mutant fibroblast cell lines, we analyzed the steady-state levels of several nuclear-encoded subunits of the OXPHOS system by immunoblotting. In fibroblasts from individuals #72425, #75191, and #76671 (F3: II-1, F4: II-4, and F5: II-2), we observed strongly reduced amounts of RCC IV. Fibroblasts from subjects #72425, #75191, and #49665 also showed reduced levels of RCC I, whereas the levels

individuals #75191 and #76671 showed a significant reduction of oxygen consumption whereas cells from individuals #49665, #72425, and #66143 presented no defective respiration. Error bar indicates 1 SD; ***$p < 0.001$.

(B) Oxygen consumption rate of fibroblast cells cultured in galactose (Gal) growth medium. The average increase of OCR from five control cells cultured in galactose-containing medium compared to glucose-containing medium was 107%. Cell lines from individuals #49665, #72425, and #66143 show significant lower increase in OCR. Lentiviral expression of wt*GTPBP3* in cells from individual #66143 significantly increases the change in OCR although it has only little effect in control cells (C6-T). Error bar indicates 1 SD; ***$p < 0.001$.

(C) Activities of respiratory chain complexes I and IV (expressed as ratio to CII activity) are decreased in individual #83904 cells transfected by electroporation with empty vector (pIRES2-EGFP) according to the manufacturer's protocol (LONZA) but are improved upon expression of *GTPBP3* cDNAs from the same plasmid. Measurements were performed as previously described.[29,30] Error bar indicates 1 SD. Activity in controls was set as 100%. **$p < 0.01$, **$p < 0.001$.

(D) Levels of GTPBP3 were reduced in cells from individuals #49665, #75191, and #66143 and elevated after transduction with wt*GTPBP3* cDNA. MRPS18B and MRPL3 served as mitochondrial loading controls.

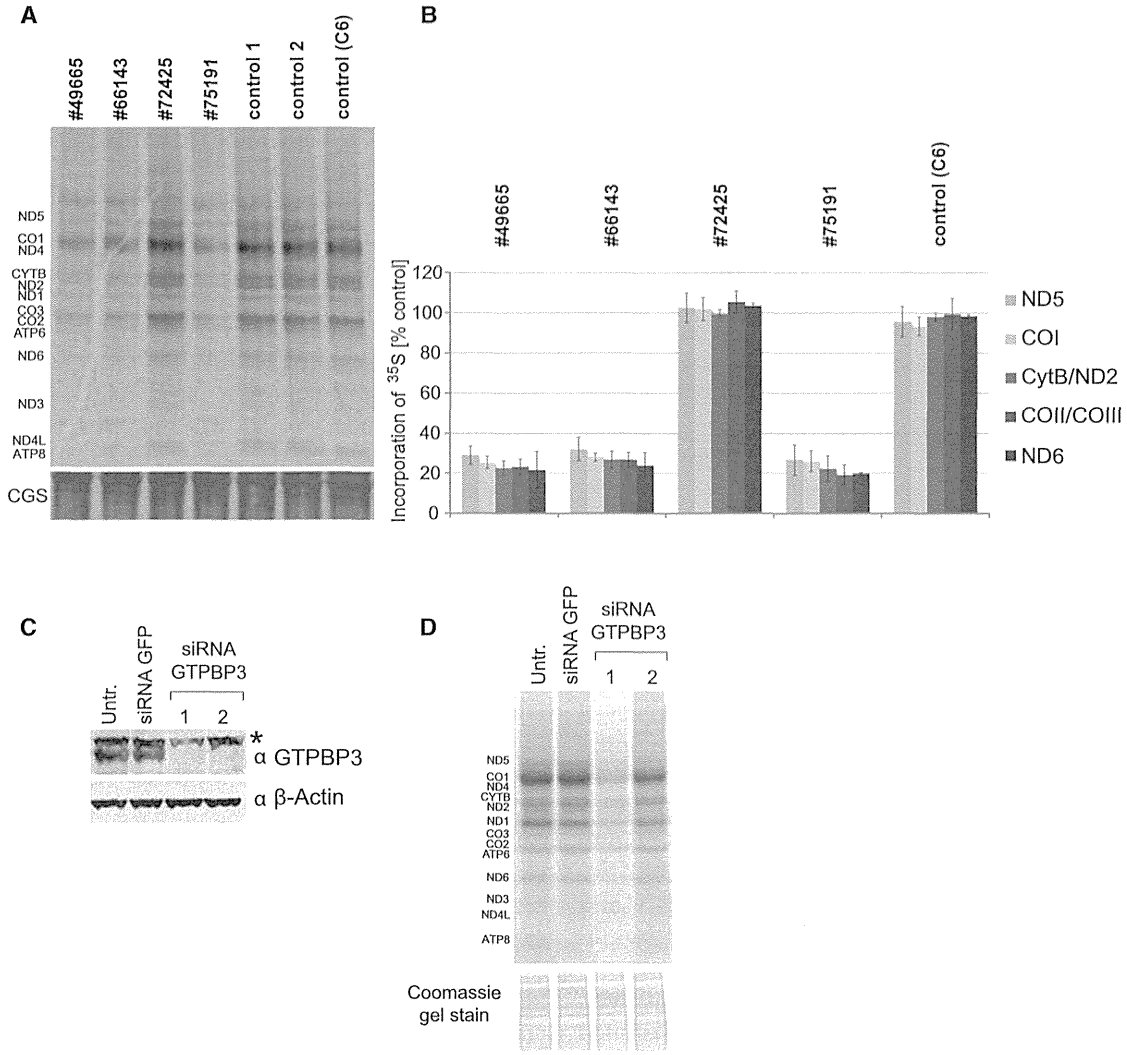

Figure 4. Analysis of Mitochondrial Protein Synthesis in Primary Fibroblasts and in HeLa Cells Treated with RNAi against GTPBP3
(A) [^{35}S]methionine metabolic labeling of mitochondrial proteins in fibroblasts. Products of mitochondrial translation were labeled with [^{35}S]methionine for 30 min, separated by a 4%–12% gradient SDS-PAGE, and visualized by autoradiography. To validate equal protein loading, a small section of the gel was stained with Coomassie (CGS). Fibroblasts from individuals #49665, #66143, and #75191 demonstrate significant inhibition of mitochondrial protein synthesis although translation in cells from individual #72425 is not affected.
(B) Quantification of radiolabelled products of mitochondrial translation. Incorporation of [^{35}S] as in (A) was quantified by ImageQuant software after exposure to a PhosphorImager screen from three independent experiments. Error bar indicates 1 SD.
(C) Downregulation of GTPBP3 in HeLa cells via RNA interference. Immunoblot analysis of total HeLa cell lysate transfected with two different siRNA to GTPBP3 show decreased level of GTPBP3 upon RNAi treatment for 6 days. siRNA to GFP was used as transfection control. Asterisk indicates nonspecific band recognized by anti-GTPBP3 antibody in HeLa cells. β-actin serves as a loading control. Two different siRNA duplexes targeting GTPBP3 were used, 1 and 2.
(D) Mitochondrial translation in HeLa cells upon GTPBP3 downregulation. HeLa cells were transfected for 6 days with siRNA against GTPBP3 and subjected to [^{35}S]methionine metabolic labeling. Inactivation of GTPBP3 leads to the reduced efficiency of mitochondrial translation. Two different siRNA duplexes targeting GTPBP3 were used, 1 and 2.

of RCC II and V remained normal in all cell lines (Figure 5). The diminished steady-state levels of respiratory chain complexes I and IV in fibroblast cell lines are in agreement with the impaired mitochondrial de novo translation rates in these cells and match the enzymatic defects identified in muscle biopsies of the same individuals.

Within an international cooperation between European (Germany, UK, Italy, France, and Belgium), Israeli, and Japanese Centers for mitochondrial disorders, we provide statistically convincing evidence for *GTPBP3* mutations leading to mitochondrial disease. To further support collaborative studies, the global mitochondrial disease community has established a Mitochondrial Disease Sequence Data Resource (MSeqDR) for common genomic data deposition and mining.

The genotype-driven analysis performed here was independent from the clinical presentation. Nevertheless, we identified common clinical features of the affected individuals that include lactic acidosis (11/11), cardiomyopathy (9/11), and neurological symptoms (6/11). The latter

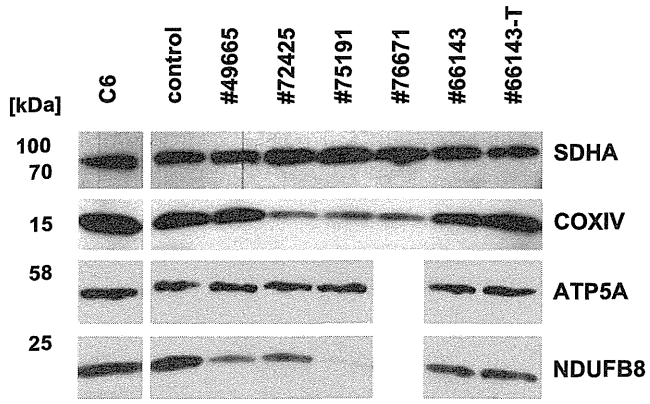

Figure 5. Immunoblot Analysis of OXPHOS Proteins in Fibroblasts

10 μg of detergent-solubilized total cell extract was subjected to immunoblot analysis of OXPHOS components. Amounts of SDHA (complex II) and ATP5A (ATPase) were unchanged in all individuals. In cells from individuals #72425, #75191, and #76671, a reduction of COXIV (complex IV) was observed. Cells from individuals #49665, #72425, and #75191 showed decreased levels of NDUFB8 (complex I). Antibodies used: mouse antibodies against SDHA (ab14715), NDUFB8 (ab110242), ATP5A (ab14748), and rabbit antibodies against COXIV (ab16056) from Abcam and rabbit anti GTPBP3 (HPA042158) from SIGMA Aldrich.

comprised symptoms such as development delay, intellectual disability, feeding difficulties, muscle hypotonia, fatigue, visual impairment, and epileptic seizures. Severity of the disease ranged from neonatal onset and death to late-infantile onset and survival into the second decade of life. Most affected individuals, however, manifested clinical symptoms before their first birthday. This is consistent with the normal cellular respiration, in organello translation, and normal levels of respiratory chain complexes reported in individuals less severely affected and the significantly reduced mitochondrial translation, respiration, and low levels of complex I and IV in those severely affected.

Modifications of the tRNA "wobble-base" in the anticodon loop are required for accurate and efficient codon recognition. The modification of position 5 (xm^5) of the U34 wobble-base of certain tRNAs is evolutionarily well conserved, although different modified side chains have been identified in different species. In mammals, mitochondria 5-taurinomethyluridine (τm^5U34) is found at the wobble-base position.[19] Based upon studies in bacteria and yeast mitochondria, GTPBP3 and MTO1 have been proposed to generate this modification in mammalian mitochondria. Although this prediction awaits direct biochemical validation, the proposed functional conservation of GTPBP3 and MTO1 has been supported by the mitochondrial localization of these proteins in human cells and by complementation of the respiratory-deficient phenotype in yeast by their mammalian homolog cDNAs.[20,21] Functional deficiency of homologs of GTPBP3 and MTO1 in bacteria and yeast mitochondria has been associated with abnormal U34 modification and consequently a reduced efficiency of translation.[21–23] Our data support an analogous activity of GTPBP3 in human mitochondria since we identified a reduced efficiency of translation in three cell lines with *GTPBP3* mutations and in cells with RNAi-mediated downregulation of GTPBP3 expression. Other groups have also reported impaired protein synthesis and reduced mitochondrial function in GTPBP3-depleted cells.[24] The defect in mitochondrial translation was a likely cause of the combined respiratory chain complex deficiency detected in muscle tissues of all but one affected individual.

Like *GTPBP3* mutations, *MTO1* mutations are also associated with hypertrophic cardiomyopathy (HCM), lactic acidosis, and combined respiratory chain deficiency. An association of *MTO1* mutations with impaired mitochondrial translation has yet to be shown for human mitochondria, but the common clinical presentation provides support for a common pathomechanism in the U34 modification for both diseases. So far, all individuals with *MTO1* mutations presented a HCM. However, nearly all of them have been specifically screened for *MTO1* mutations based on the clinical presentation of a HCM. Clinical and MRI signs of brain involvement are found for both *GTPBP3* and *MTO1* cases. The genotype-driven investigation presented here identified individuals with lactic acidosis, developmental delay, and MRI involvement of thalamus, putamen, and brainstem but without HCM. It can be expected that the clinical spectrum associated with MTO1 deficiency will also broaden, with more subjects being genome-wide investigated. In a very recent study, Taylor et al. indeed reported a case subject with *MTO1* mutations and central neurological features who did not have a cardiomyopathy.[25]

Our study highlights that defects in mitochondrial translation, probably owing to incorrect posttranscriptional modification of mt-tRNAs, are an important contributory factor to the spectrum of human mitochondrial disease. Recent data have suggested that more than 7% of all mt-tRNA residues undergo posttranscriptional modification, with close to 30 different modifications so far described.[4] Therefore, it is expected that future WES analyses of individuals clinically diagnosed with mitochondriopathy will reveal further mutations within genes coding for mt-tRNA modifiers. Indeed, in addition to the aforementioned mutations in *MTO1* and *TRMU*, mutations in *PUS1* (MIM 608109) (which introduces pseudouridine [Ψ] at base positions 27, 28, and 29 in several mt-tRNAs) have been reported in subjects affected with mitochondrial myopathy and sideroblastic anemia (MLASA)[26] (MIM 600462) and very recent studies have identified mutations in *TRIT1* (which is responsible for i^6A37 modification of a subset of mt-tRNAs) in individuals with severe combined mitochondrial respiratory chain defects.[27] Furthermore, mtDNA mutations in mt-tRNA genes, which are a very frequent cause of human respiratory chain deficiencies (MITOMAP), might also affect mt-tRNA modification. Related to the present study, it has been reported that τm^5U34 is not present in mt-tRNALeu^{UUR} harboring the m.3243A>G mutation (or other pathological mutations) responsible for mitochondrial encephalopathy, lactic

acidosis, and stroke-like episodes (MELAS) (MIM 540000). The absence of τm^5U34 has been suggested to be responsible for the mitochondrial translation defect in these subjects.[28] These results imply that deficiency of mt-tRNA modification plays a critical role in the molecular pathogenesis of human respiratory chain disease. Further studies of these pathways, such as analysis of tissue-specific regulation of mt-tRNA-modifying enzymes, might help to explain the clinical heterogeneity observed for mitochondrial diseases caused by mutations in mt-tRNA genes.

In conclusion, this study shows a mitochondrial translation disorder with a broad spectrum of clinical presentations, which emphasizes the importance of post-transcriptional modification of mitochondrial tRNAs for proper mitochondrial function.

Supplemental Data

Supplemental Data include four figures and can be found with this article online at http://dx.doi.org/10.1016/j.ajhg.2014.10.017.

Acknowledgments

We thank C. Terrile, M. Borzes, and C. Fischer for technical support and F. Miyake and T. Wada for referral of sample materials. This work was supported by the Deutsche Forschungsgemeinschaft within the framework of the Munich Cluster for Systems Neurology (EXC 1010 SyNergy), the German Bundesministerium für Bildung und Forschung (BMBF) through funding of the E-Rare project GENOMIT (01GM1207 for T.M. and H.P., 2011-RARE-005-03 for A.R. and M.D.M., J41J11000420001 for M.Z., and FWF I 920-B13 for J.A.M.), German Network for Mitochondrial Disorders (mitoNET 01GM1113C for T.M., H.P., and P.F. and 01GM1113A for T.K.), the German Center for Heart Research (Z76010017300 and Z56010015300 for T.M.), European Commission 7th Framework Program (Project N261123 GEUVADIS), Medical Research Council, UK (MC_U105697135 for T.J.N., J.R., S.F.P., C.A.P., and M.M.), Wellcome Trust Strategic Award (096919/Z/11/Z for R.W.T. and P.F.C.), MRC Centre for Neuromuscular Diseases (G0601943), UK NHS Highly Specialised "Rare Mitochondrial Disorders of Adults and Children" Service for R.W.T. and P.F.C., Fund for Scientific Research Belgium (FWO, contract number G.0200.10 for A.V., J.S., and R.V.C.), Fondazione Telethon (GGP11011 and GPP10005), Italian Ministry of Health (GR2010-2316392), CARIPLO (2011/0526), Pierfranco and Luisa Mariani Foundation, and Italian Association of Mitochondrial Disease Patients and Families (Mitocon) to D.G., F.I., E.L., and M.Z., Research Program of Innovative Cell Biology by Innovative Technology (Cell Innovation), Grant-in-Aid for the Development of New Technology from The Promotion and Mutual Aid Corporation for Private Schools of Japan from MEXT for Y.O., Grants-in-Aid for the Research on Intractable Diseases from the Ministry of Health, Labour and Welfare of Japan for A.O., Kawano Masanori Memorial Public Interest Incorporated Foundation for Promotion of Pediatrics for K. Murayama, Association Française contre les Myopathies (AFM) for A.R. and M.D.M., and Fellowship from the AFM (16615 for M.D.M.).

Received: July 30, 2014
Accepted: October 29, 2014
Published: November 26, 2014

Web Resources

The URLs for data presented herein are as follows:

MITOMAP, http://www.mitomap.org/MITOMAP
MSeqDR, https://mseqdr.org/
Online Mendelian Inheritance in Man (OMIM), http://www.omim.org/
Predotar, https://urgi.versailles.inra.fr/predotar/predotar.html
PSORTII Prediction, http://psort.hgc.jp/form2.html
RefSeq, http://www.ncbi.nlm.nih.gov/RefSeq

References

1. Boczonadi, V., and Horvath, R. (2014). Mitochondria: impaired mitochondrial translation in human disease. Int. J. Biochem. Cell Biol. *48*, 77–84.
2. Osawa, S. (1995). Evolution of the Genetic Code (Washington, DC: ASM Press).
3. Suzuki, T. (2005). Biosynthesis and function of tRNA wobble modifications. Top. Curr. Genet. *12*, 23–69.
4. Suzuki, T., and Suzuki, T. (2014). A complete landscape of post-transcriptional modifications in mammalian mitochondrial tRNAs. Nucleic Acids Res. *42*, 7346–7357.
5. Colby, G., Wu, M., and Tzagoloff, A. (1998). MTO1 codes for a mitochondrial protein required for respiration in paromomycin-resistant mutants of *Saccharomyces cerevisiae*. J. Biol. Chem. *273*, 27945–27952.
6. Yokoyama, S., Watanabe, T., Murao, K., Ishikura, H., Yamaizumi, Z., Nishimura, S., and Miyazawa, T. (1985). Molecular mechanism of codon recognition by tRNA species with modified uridine in the first position of the anticodon. Proc. Natl. Acad. Sci. USA *82*, 4905–4909.
7. Björk, G.R., Huang, B., Persson, O.P., and Byström, A.S. (2007). A conserved modified wobble nucleoside (mcm5s2U) in lysyl-tRNA is required for viability in yeast. RNA *13*, 1245–1255.
8. Yarham, J.W., Elson, J.L., Blakely, E.L., McFarland, R., and Taylor, R.W. (2010). Mitochondrial tRNA mutations and disease. Wiley Interdiscip. Rev. RNA *1*, 304–324.
9. Zeharia, A., Shaag, A., Pappo, O., Mager-Heckel, A.-M., Saada, A., Beinat, M., Karicheva, O., Mandel, H., Ofek, N., Segel, R., et al. (2009). Acute infantile liver failure due to mutations in the TRMU gene. Am. J. Hum. Genet. *85*, 401–407.
10. Ghezzi, D., Baruffini, E., Haack, T.B., Invernizzi, F., Melchionda, L., Dallabona, C., Strom, T.M., Parini, R., Burlina, A.B., Meitinger, T., et al. (2012). Mutations of the mitochondrial-tRNA modifier MTO1 cause hypertrophic cardiomyopathy and lactic acidosis. Am. J. Hum. Genet. *90*, 1079–1087.
11. Baruffini, E., Dallabona, C., Invernizzi, F., Yarham, J.W., Melchionda, L., Blakely, E.L., Lamantea, E., Donnini, C., Santra, S., Vijayaraghavan, S., et al. (2013). MTO1 mutations are associated with hypertrophic cardiomyopathy and lactic acidosis and cause respiratory chain deficiency in humans and yeast. Hum. Mutat. *34*, 1501–1509.
12. Elstner, M., Andreoli, C., Klopstock, T., Meitinger, T., and Prokisch, H. (2009). The mitochondrial proteome database: MitoP2. Methods Enzymol. *457*, 3–20.
13. Invernizzi, F., D'Amato, I., Jensen, P.B., Ravaglia, S., Zeviani, M., and Tiranti, V. (2012). Microscale oxygraphy reveals OXPHOS impairment in MRC mutant cells. Mitochondrion *12*, 328–335.
14. Petrova-Benedict, R., Buncic, J.R., Wallace, D.C., and Robinson, B.H. (1992). Selective killing of cells with oxidative

defects in galactose medium: a screening test for affected patient fibroblasts. J. Inherit. Metab. Dis. *15*, 943–944.
15. Robinson, B.H., Petrova-Benedict, R., Buncic, J.R., and Wallace, D.C. (1992). Nonviability of cells with oxidative defects in galactose medium: a screening test for affected patient fibroblasts. Biochem. Med. Metab. Biol. *48*, 122–126.
16. Danhauser, K., Iuso, A., Haack, T.B., Freisinger, P., Brockmann, K., Mayr, J.A., Meitinger, T., and Prokisch, H. (2011). Cellular rescue-assay aids verification of causative DNA-variants in mitochondrial complex I deficiency. Mol. Genet. Metab. *103*, 161–166.
17. Kornblum, C., Nicholls, T.J., Haack, T.B., Schöler, S., Peeva, V., Danhauser, K., Hallmann, K., Zsurka, G., Rorbach, J., Iuso, A., et al. (2013). Loss-of-function mutations in MGME1 impair mtDNA replication and cause multisystemic mitochondrial disease. Nat. Genet. *45*, 214–219.
18. Haack, T.B., Kopajtich, R., Freisinger, P., Wieland, T., Rorbach, J., Nicholls, T.J., Baruffini, E., Walther, A., Danhauser, K., Zimmermann, F.A., et al. (2013). ELAC2 mutations cause a mitochondrial RNA processing defect associated with hypertrophic cardiomyopathy. Am. J. Hum. Genet. *93*, 211–223.
19. Suzuki, T., Suzuki, T., Wada, T., Saigo, K., and Watanabe, K. (2002). Taurine as a constituent of mitochondrial tRNAs: new insights into the functions of taurine and human mitochondrial diseases. EMBO J. *21*, 6581–6589.
20. Li, X., and Guan, M.-X. (2002). A human mitochondrial GTP binding protein related to tRNA modification may modulate phenotypic expression of the deafness-associated mitochondrial 12S rRNA mutation. Mol. Cell. Biol. *22*, 7701–7711.
21. Li, X., Li, R., Lin, X., and Guan, M.-X. (2002). Isolation and characterization of the putative nuclear modifier gene MTO1 involved in the pathogenesis of deafness-associated mitochondrial 12 S rRNA A1555G mutation. J. Biol. Chem. *277*, 27256–27264.
22. Wang, X., Yan, Q., and Guan, M.-X. (2010). Combination of the loss of cmnm5U34 with the lack of s2U34 modifications of tRNALys, tRNAGlu, and tRNAGln altered mitochondrial biogenesis and respiration. J. Mol. Biol. *395*, 1038–1048.
23. Murphy, F.V., 4th, Ramakrishnan, V., Malkiewicz, A., and Agris, P.F. (2004). The role of modifications in codon discrimination by tRNA(Lys)UUU. Nat. Struct. Mol. Biol. *11*, 1186–1191.
24. Villarroya, M., Prado, S., Esteve, J.M., Soriano, M.A., Aguado, C., Pérez-Martínez, D., Martínez-Ferrandis, J.I., Yim, L., Victor, V.M., Cebolla, E., et al. (2008). Characterization of human GTPBP3, a GTP-binding protein involved in mitochondrial tRNA modification. Mol. Cell. Biol. *28*, 7514–7531.
25. Taylor, R.W., Pyle, A., Griffin, H., Blakely, E.L., Duff, J., He, L., Smertenko, T., Alston, C.L., Neeve, V.C., Best, A., et al. (2014). Use of whole-exome sequencing to determine the genetic basis of multiple mitochondrial respiratory chain complex deficiencies. JAMA *312*, 68–77.
26. Bykhovskaya, Y., Casas, K., Mengesha, E., Inbal, A., and Fischel-Ghodsian, N. (2004). Missense mutation in pseudouridine synthase 1 (PUS1) causes mitochondrial myopathy and sideroblastic anemia (MLASA). Am. J. Hum. Genet. *74*, 1303–1308.
27. Yarham, J.W., Lamichhane, T.N., Pyle, A., Mattijssen, S., Baruffini, E., Bruni, F., Donnini, C., Vassilev, A., He, L., Blakely, E.L., et al. (2014). Defective i6A37 modification of mitochondrial and cytosolic tRNAs results from pathogenic mutations in TRIT1 and its substrate tRNA. PLoS Genet. *10*, e1004424.
28. Yasukawa, T., Suzuki, T., Ueda, T., Ohta, S., and Watanabe, K. (2000). Modification defect at anticodon wobble nucleotide of mitochondrial tRNAs(Leu)(UUR) with pathogenic mutations of mitochondrial myopathy, encephalopathy, lactic acidosis, and stroke-like episodes. J. Biol. Chem. *275*, 4251–4257.
29. Rustin, P., Chretien, D., Bourgeron, T., Gérard, B., Rötig, A., Saudubray, J.M., and Munnich, A. (1994). Biochemical and molecular investigations in respiratory chain deficiencies. Clin. Chim. Acta *228*, 35–51.
30. Rustin, P., Chretien, D., Bourgeron, T., Wucher, A., Saudubray, J.M., Rotig, A., and Munnich, A. (1991). Assessment of the mitochondrial respiratory chain. Lancet *338*, 60.

The American Journal of Human Genetics, Volume *95*
Supplemental Data

Mutations in *GTPBP3* Cause a Mitochondrial Translation Defect Associated with Hypertrophic Cardiomyopathy, Lactic Acidosis, and Encephalopathy

Robert Kopajtich, Thomas J. Nicholls, Joanna Rorbach, Metodi D. Metodiev, Peter Freisinger, Hanna Mandel, Arnaud Vanlander, Daniele Ghezzi, Rosalba Carrozzo, Robert W. Taylor, Klaus Marquard, Kei Murayama, Thomas Wieland, Thomas Schwarzmayr, Johannes A. Mayr, Sarah F. Pearce, Christopher A. Powell, Ann Saada, Akira Ohtake, Federica Invernizzi, Eleonora Lamantea, Ewen W. Sommerville, Angela Pyle, Patrick F. Chinnery, Ellen Crushell, Yasushi Okazaki, Masakazu Kohda, Yoshihito Kishita, Yoshimi Tokuzawa, Zahra Assouline, Marlène Rio, François Feillet, Bénédict Mousson de Camaret, Dominique Chretien, Arnold Munnich, Björn Menten, Tom Sante, JoélSmet, Luc Régal, Abraham Lorber, Asaad Khoury, Massimo Zeviani, Tim M. Strom, Thomas Meitinger, Enrico S. Bertini, Rudy Van Coster, Thomas Klopstock, Agnès Rötig, Tobias B. Haack, Michal Minczuk, and Holger Prokisch

Figure S1

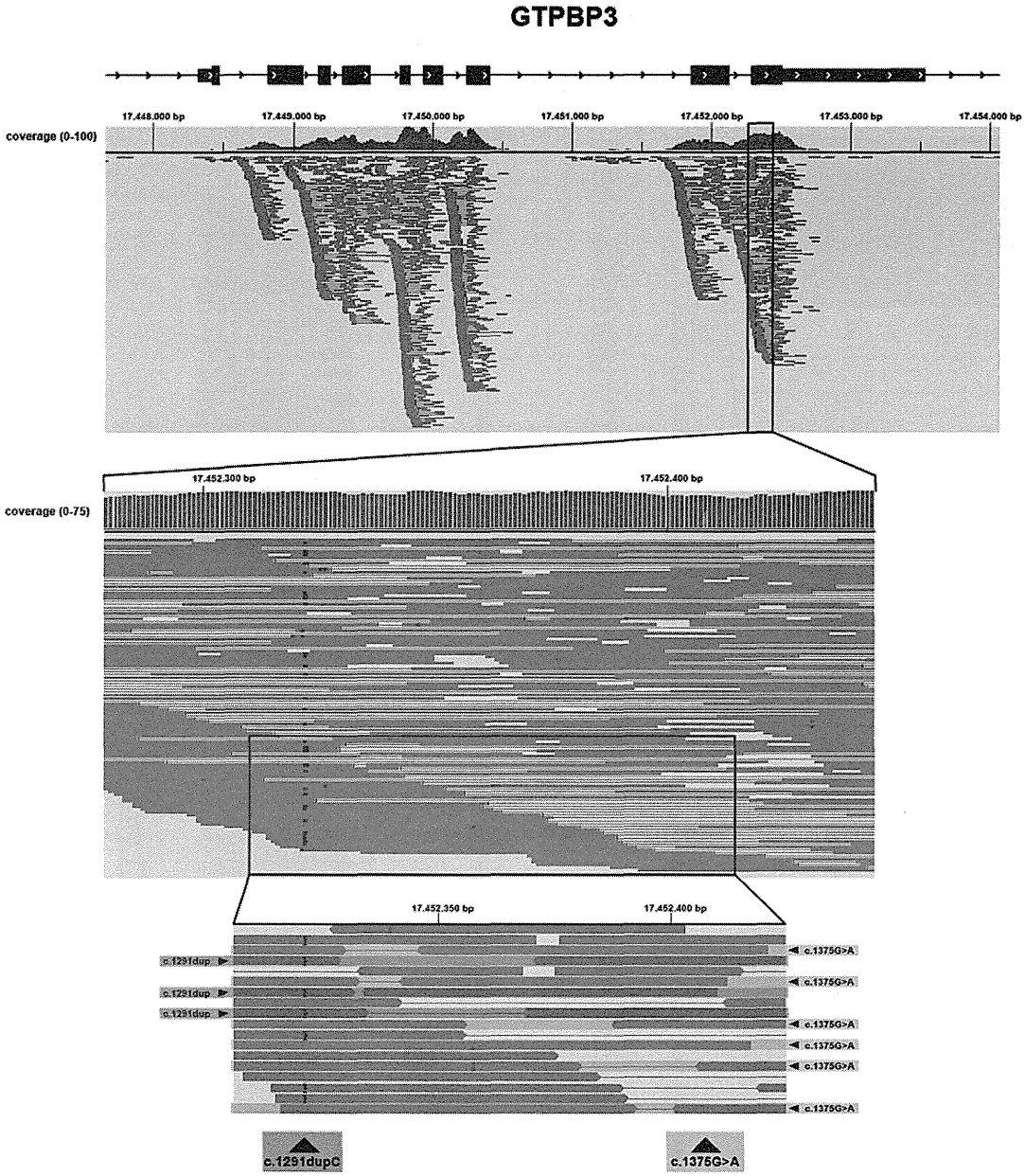

Figure S1) Segregation analysis in family F1 in WES data

The two mutations identified in family F1 (c.1291dupC and c.1375G>A) are only separated by 97 bp which allowed analysis of both alleles despite the lack of parental material. 13 paired sequence reads were identified which covered the region of both variants. All reads contained either of the two mutations demonstrating a compound heterozygous status of the two variants. Figure S1 shows three sequence reads containing the c.1291dupC variant and five reads containing the c.1375G>A variant.

Figure S2

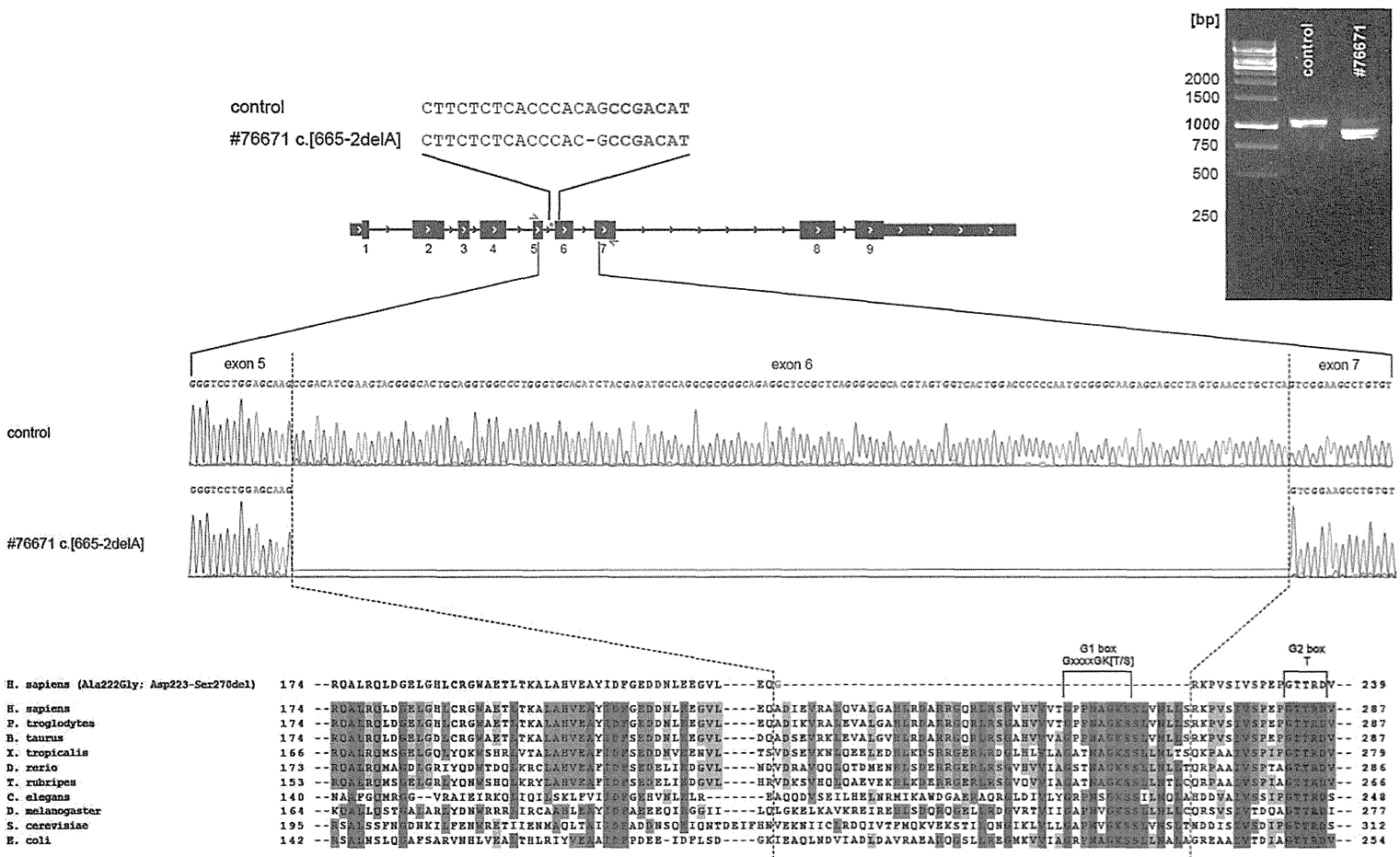

Figure S2) Splice site mutation in individual #76671 causes skipping of exon 6

Analysis of cDNA derived from fibroblasts of individual #76671 yielded a smaller than expected PCR product, indicating alternative splicing. Sanger sequencing revealed that the c.665-2delA mutation affects the conserved splice acceptor site. The splice acceptor upstream of exon 7 is alternatively used, yielding a mature mRNA that lacks exon 6. The resulting protein product is predicted to contain a 1 amino acid exchange followed by a 48 amino acid deletion (p.Ala322Gly; Asp223-270del).

Figure S3

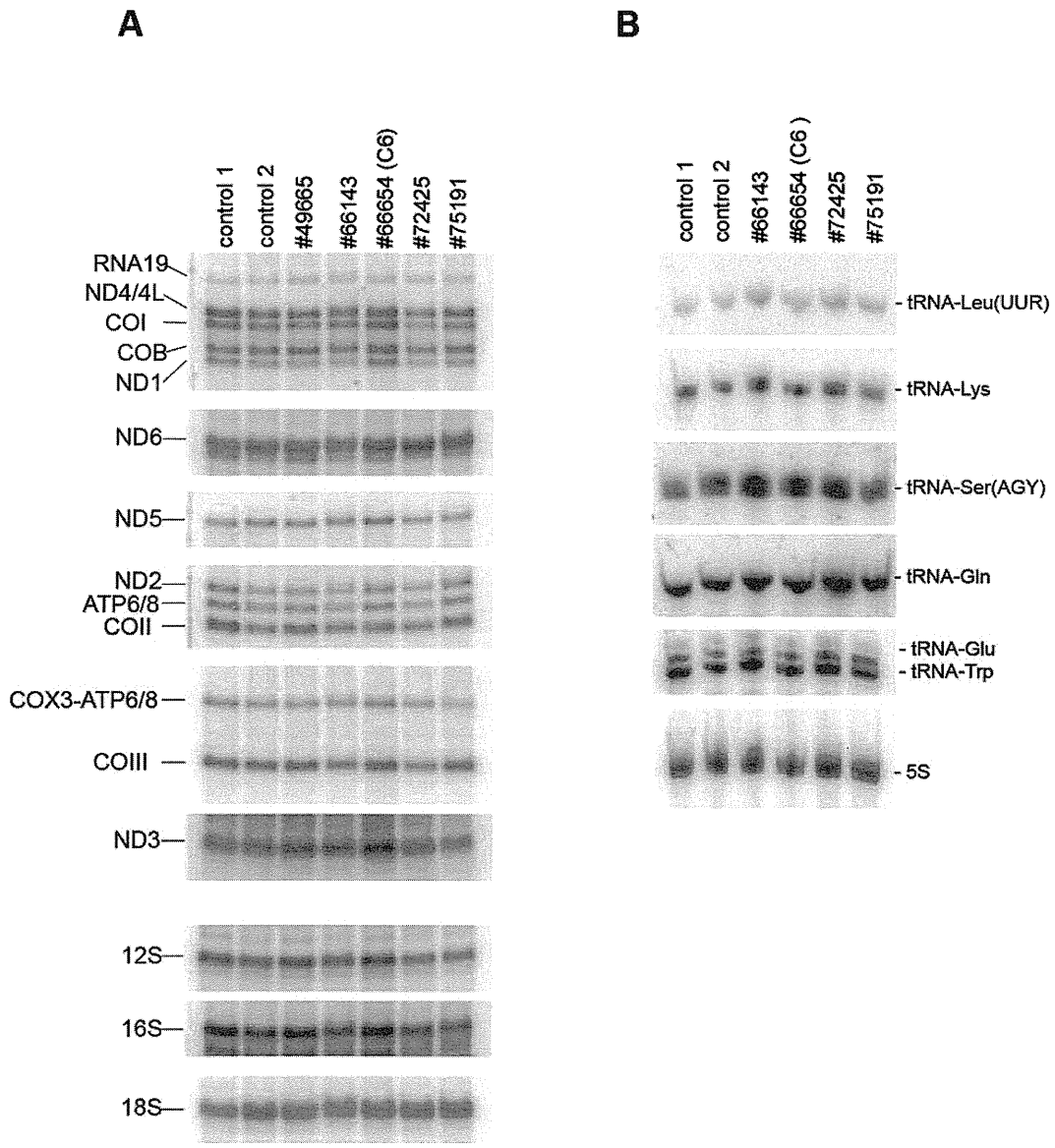

Figure S3) Northern blot analysis of the steady-state levels of mitochondrial transcripts in GTPBP3 patient fibroblasts.

A) Northern blot analysis of total RNA isolated from the *GTPBP3* patient or control primary fibroblasts. The blots were probed with the mt-mRNA- and mt-rRNA-specific probes as indicated. The cytosolic 18S rRNA was used as a loading control.

B)) High-resolution Northern blot analysis of total RNA isolated from the *GTPBP3* patient or control primary fibroblasts. The blots were probed with the mt-tRNA -specific probes as indicated. The cytosolic 5S rRNA was used as a loading control.

Figure S4

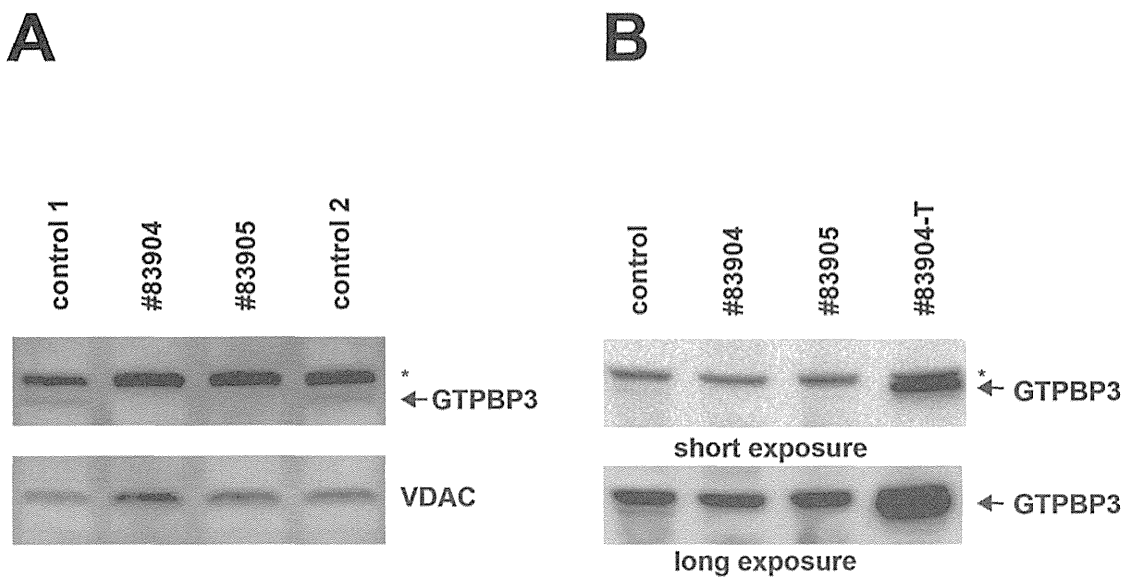

Figure S4) Analysis of GTPBP3 protein levels in patient fibroblasts

A) Immunoblot analysis of GTPBP3 protein levels in fibroblasts from affected individuals #83904 and #83905 from family F9. VDAC served as a mitochondrial loading control. (Asterics indicates a non-specific band.)

B) Comparison of the electrophoretic migration of GTPBP3 in un-transfected cells (lane control) and cells derived from one of the affected individuals transfected with a plasmid (pIRES2-EGFP) for *GTPBP3* cDNA expression (lane #83904-T). (Asterics indicates a non-specific band.)

Annals of Clinical and Translational Neurology
Open Access
ANA American Neurological Association

RESEARCH PAPER

New *MT-ND6* and *NDUFA1* mutations in mitochondrial respiratory chain disorders

Natsumi Uehara[1,2], Masato Mori[3], Yoshimi Tokuzawa[1], Yosuke Mizuno[1], Shunsuke Tamaru[1], Masakazu Kohda[1,4], Yohsuke Moriyama[1], Yutaka Nakachi[1,4], Nana Matoba[4], Tetsuro Sakai[5], Taro Yamazaki[5], Hiroko Harashima[5], Kei Murayama[6], Keisuke Hattori[7], Jun-Ichi Hayashi[7], Takanori Yamagata[3], Yasunori Fujita[8], Masafumi Ito[8], Masashi Tanaka[9], Ken-ichi Nibu[2], Akira Ohtake[5] & Yasushi Okazaki[1,4]

[1]Division of Functional Genomics & Systems Medicine, Research Center for Genomic Medicine, Saitama Medical University, Hidaka, Japan
[2]Department of Otolaryngology-Head and Neck Surgery, Kobe University Graduate School of Medicine, Kobe, Japan
[3]Department of Pediatrics, Jichi Medical University, Shimotsuke, Japan
[4]Division of Translational Research, Research Center for Genomic Medicine, Saitama Medical University, Hidaka, Japan
[5]Department of Pediatrics, Faculty of Medicine, Saitama Medical University, Moroyama-machi, Japan
[6]Department of Metabolism, Chiba Children's Hospital, Chiba, Japan
[7]Faculty of Life and Environmental Sciences, University of Tsukuba, Tsukuba, Japan
[8]Research Team for Mechanism of Aging, Tokyo Metropolitan Institute of Gerontology, Itabashi, Japan
[9]Department of Genomics for Longevity and Health, Tokyo Metropolitan Institute of Gerontology, Itabashi, Japan

Correspondence
Yasushi Okazaki, Division of Functional Genomics & Systems Medicine, Research Center for Genomic Medicine, Saitama Medical University, 1397-1 Yamane, Hidaka, Saitama 350-1241, Japan. Tel: +81-42-984-0448; Fax: +81-42-984-0449; E-mail: okazaki@saitama-med.ac.jp
Akira Ohtake, Department of Pediatrics, Faculty of Medicine, Saitama Medical University, 38 Morohongo, Moroyama-machi, Iruma-gun, Saitama 350-0495, Japan. Tel: +81-49-276-1220; Fax: +81-49-276-1790; E-mail: akira_oh@saitama-med.ac.jp

Funding Information
This study was supported in part by a grant from the Research Program of Innovative Cell Biology by Innovative Technology (Cell Innovation), a Grant-in-Aid for the Development of New Technology from The Promotion and Mutual Aid Corporation for Private Schools of Japan from MEXT (to Y. O.), a Grant-in-Aid research grants for Scientific Research (A-22240072, B-21390459, A-25242062) from the Ministry of Education, Culture, Sports, Science, and Technology (MEXT) of Japan to M. T., and a Grant-in-Aids (H23-016, H23-119, and H24-005) for the Research on Intractable Diseases (Mitochondrial Disease) from the Ministry of Health, Labour and Welfare (MHLW) of Japan to M. T. and A. O., and a Grant-in-Aids (H23-001, H24-017, H24-071) for the Research on Intractable Diseases from the Ministry of Health, Labour and Welfare (MHLW) of Japan to A. O.

Abstract

Objective: Mitochondrial respiratory chain disorder (MRCD) is an intractable disease of infants with variable clinical symptoms. Our goal was to identify the causative mutations in MRCD patients. **Methods**: The subjects were 90 children diagnosed with MRCD by enzyme assay. We analyzed whole mitochondrial DNA (mtDNA) sequences. A cybrid study was performed in two patients. Whole exome sequencing was performed for one of these two patients whose mtDNA variant was confirmed as non-pathogenic. **Results**: Whole mtDNA sequences identified 29 mtDNA variants in 29 patients (13 were previously reported, the other 13 variants and three deletions were novel). The remaining 61 patients had no pathogenic mutations in their mtDNA. Of the 13 patients harboring unreported mtDNA variants, we excluded seven variants by manual curation. Of the remaining six variants, we selected two Leigh syndrome patients whose mitochondrial enzyme activity was decreased in their fibroblasts and performed a cybrid study. We confirmed that m.14439G>A (*MT-ND6*) was pathogenic, while m.1356A>G (*mitochondrial 12S rRNA*) was shown to be a non-pathogenic polymorphism. Exome sequencing and a complementation study of the latter patient identified a novel c.55C>T hemizygous missense mutation in the nuclear-encoded gene *NDUFA1*. **Interpretation**: Our results demonstrate that it is important to perform whole mtDNA sequencing rather than only typing reported mutations. Cybrid assays are also useful to diagnose the pathogenicity of mtDNA variants, and whole exome sequencing is a powerful tool to diagnose nuclear gene mutations as molecular diagnosis can provide a lead to appropriate genetic counseling.

Received: 11 December 2013; Revised: 11 February 2014; Accepted: 18 March 2014

***Annals of Clinical and Translational Neurology* 2014; 1(5): 361–369**

doi: 10.1002/acn3.59

Introduction

The mitochondrial respiratory chain (RC) is a pathway for vital energy generation in which ATP is generated as a form of energy by the substrates generated from glycolysis and β-oxidation. The pathway is composed of five multi-enzyme complexes (complexes I–V), two electron carriers, a quinone (coenzyme Q), and a small hem-containing protein (cytochrome c) that are located in the inner mitochondrial membrane. These RC complexes are formed from subunits encoded by both mitochondrial DNA (mtDNA) and nuclear DNA (nDNA), with the exception of complex II, which is entirely encoded by nDNA.

mtDNA is a circular double-stranded DNA molecule ~16 kb in length that encodes 37 genes comprising 13 proteins, 22 mitochondrial tRNAs, and 2 rRNAs.[1,2] Defects in mitochondrial function are associated with numerous neurodegenerative diseases, such as Parkinson's disease, Alzheimer's disease, and Huntington's disease, and, in particular with mitochondrial respiratory chain disorder (MRCD). MRCD is genetically, clinically, and biochemically heterogeneous, and it can give rise to any symptoms, in any organs or tissues, at any age and with any mode of inheritance.[3] One in 5000 births is a conservative realistic estimate for the minimum birth prevalence of MRCD.[4] Especially in children, MRCD is an intractable disease and can be regarded as the most common group of inborn errors of metabolism.[5,6]

Some MRCD patients have typical clinical findings that are caused by specific point mutations or large deletions of mtDNA. Typical clinical features include mitochondrial myopathy, encephalopathy, lactic acidosis, and stroke-like episodes (MELAS), myoclonus epilepsy associated with ragged-red fibers (MERRF), Leber's hereditary optic neuropathy (LHON), and chronic progressive external ophthalmoplegia (CPEO).[2] Although mtDNA mutations or deletions are usually found in adults showing typical clinical findings, they account for only a minority of children with MRCD. Therefore, the diagnosis of MRCD in children by screening known mtDNA mutations is rather difficult.[7] Hence, a combination of general biochemical study, histological study, and genetic analysis is essential for the diagnosis of MRCD, especially in children.[6]

In this study, we performed whole mtDNA sequencing for 90 children diagnosed with MRCD by RC enzyme assay with the aim of identifying causative mtDNA mutations.

Subjects, Materials, and Methods

Patients

Ninety Japanese pediatric patients diagnosed with MRCD and without characteristic clinical syndromes were studied. The primary diagnosis for these patients was definite or probable MRCD based on the criteria of Bernier et al.,[8] and a mitochondrial RC residual enzyme activity of <20% in a tissue, <30% in a fibroblast cell line, or <30% in two or more tissues (Data S1). Informed consent was obtained from the patients and their families before participation in the study.

Patient summaries are shown in Tables 1, 2. The details of the two patients studied in the cybrid assay are as follows: Patient (Pt) 377 is a 1-year-old girl born after a normal pregnancy to non-consanguineous parents. She has a normal brother and sister. She was hospitalized with gait difficulties at the age of 1 year. Blood lactate levels were high. Brain magnetic resonance imaging (MRI)

Table 1. Distribution of mtDNA variants and clinical features.

Characteristics		Non-pathogenic mutations	Low probability variants	New pathogenic deletions	Known variants	Total
Number of subjects		61 (100%)	13 (100%)	3 (100%)	13 (100%)	90 (100%)
No consanguinity		57 (93%)	12 (92%)	3 (100%)	11 (85%)	84 (93%)
Age at onset	≤1 y.o.	54 (89%)	10 (77%)	3 (100%)	9 (69%)	76 (84%)
Status	Alive	33 (54%)	7 (54%)	1 (33%)	11 (85%)	53 (59%)
	Dead	28 (46%)	6 (46%)	2 (67%)	2 (15%)	37 (41%)
Sex	Female	30 (49%)	3 (23%)	2 (67%)	6 (46%)	41 (46%)
	Male	31 (51%)	10 (77%)	1 (33%)	7 (54%)	49 (54%)

y.o., years old.

Table 2. Summary of unreported mutations and deletions.

Patient ID	Age at onset	Clinical diagnosis	Enzyme assay (organ)	mtDNA variation	Locus	Heteroplasmy
377	1 year	LD	1 (Fb)	m.14439G>A	*ND6*	Homo (Fb)
190	1 year 6 months	LD	1,4 (M)	m.11246G>A	*ND4*	73% (fb)
508	0 days	SIDS	1 (Hep,Car)	m.4638A>G	*ND2*	86% (Fb), 0% (Hep, Car)
004	0 months	MC	1 (Fb)	m.5537A>G[1]	*tRNATrp*	27.4% (Fb)
271	0 months	ELBW	1 (Hep)	m.10045T>C	*tRNAGly*	Homo (hep)
312[2]	5 years	LD	1 (Fb) probably	m.1356A>G	*12S rRNA*	66% (Fb)
372	2 days	LIMD	1 (Hep)	Deletion (3424 bp) nt12493-15916		65.7% (Fb), 89.9% (Hep)
336	11 months	HD	1 (Hep)	Deletion (6639 bp) nt7734-14372		9.2% (Fb), 92.6% (Hep)
390	0 days	MC	1,4 (M,Hep)	Deletion (5424 bp) nt8574-13997		44.9% (Fb), 86.4% (Hep)

LIMD, lethal infantile mitochondrial disorder; HD, hepatic disease; LD, Leigh's disease; MC, mitochondrial cytopathy; SIDS, sudden infant death syndrome; ELBW, extremely low birth weight infant; Fb, fibroblast; Hep, liver; Car, heart; M, muscle.
[1]Expected to be causative because of the other reported mutation on the same position.
[2]m.1356A>G was confirmed as non-pathogenic and nDNA mutation was identified in Pt312.

showed bilateral and symmetrical hyperintensity foci in the basal ganglia. She developed progressive motor regression and became bedridden. Pt312 is a 5-year-old boy born after 36 weeks' gestation following a normal pregnancy to non-consanguineous parents. His birth weight was 2154 g. He has a sister who is his fraternal twin. At 5 months of age, his parents noticed hypotonia and nystagmus. At 10 months of age, he had generalized epilepsy and blood lactate and his pyruvate levels were high. A brain MRI revealed symmetrical high T2 signals in the midbrain.

Whole mtDNA sequencing and detection of variants

Genomic DNA (gDNA) was extracted from skin fibroblasts (Data S1), blood, liver, and cardiac muscle using either phenol/chloroform- or column-based extraction. Whole mtDNA was first polymerase chain reaction (PCR)-amplified as two separate large amplicons (LA1 and LA2) avoiding the nonspecific amplifications from nDNA.[9] Second-round PCR was performed using 46 primer pairs (mitoSEQrTM; Applied Biosystems, Carlsbad, CA) and the LA1 and LA2 amplicon mixture from first-round PCR as a template. PCR conditions were as follows: first-round PCR was performed in a reaction mixture containing 0.2 mmol/L of each dNTP, 0.25 U of Takara Ex Taq (Takara Bio, Shiga, Japan), 1× Ex Taq Buffer, 0.3 μmol/L of each primer, and extracted gDNA in a total volume of 50 μL. Initial denaturation was performed at 94°C for 2 min, followed by 30 cycles of 94°C for 20 sec, 60°C for 20 sec, and 72°C for 5 min, with a final extension at 72°C for 11 min. Second-round PCR was performed in a reaction mixture as above except with a 10,000-fold dilution of LA1 amplicon and a 100-fold dilution of LA2 amplicon (total volume of the PCR reaction, 10 μL). Initial denaturation was performed at 96°C for 5 min, followed by 30 cycles of 94°C for 30 sec, 60°C for 45 sec, and 72°C for 45 sec, with a final extension at 72°C for 10 min.

First- and second-round PCR products were separated by 1% and 2% agarose gels, respectively, then 10 μL of second-round PCR products were incubated with 1 μL of ExoSAP-IT reagent (GE Healthcare UK Ltd., Bucks, U.K.) at 37°C for 30 min to degrade remaining primers and nucleotides. The ExoSAP-IT reagent was then inactivated by incubating at 75°C for 15 min. PCR products were sequenced using a BigDye Terminator v3.1 cycle sequencing kit (Applied Biosystems) and an ABI3130xl Genetic Analyzer (Applied Biosystems). Sequence data were compared with the revised Cambridge sequence (GenBank Accession No. NC_012920.1) and sequences present in MITOMAP (http://mitomap.org/MITOMAP) and mtSNP (http://mtsnp.tmig.or.jp/mtsnp/index_e.shtml) using SeqScape software (Applied Biosystems). Whole mtDNA sequencing of seven samples was obtained using an Ion PGM™ sequencer (Life Technologies Corporation, Carlsbad, CA).

Characterization of mtDNA deletions

We searched for mtDNA deletions by focusing on the size of first-round PCR products in agarose electrophoresis. If PCR products were smaller than controls, we suspected mtDNA deletion and performed further analysis. The smaller PCR products were recovered from the gel and amplified by second-round PCR, as described above, and

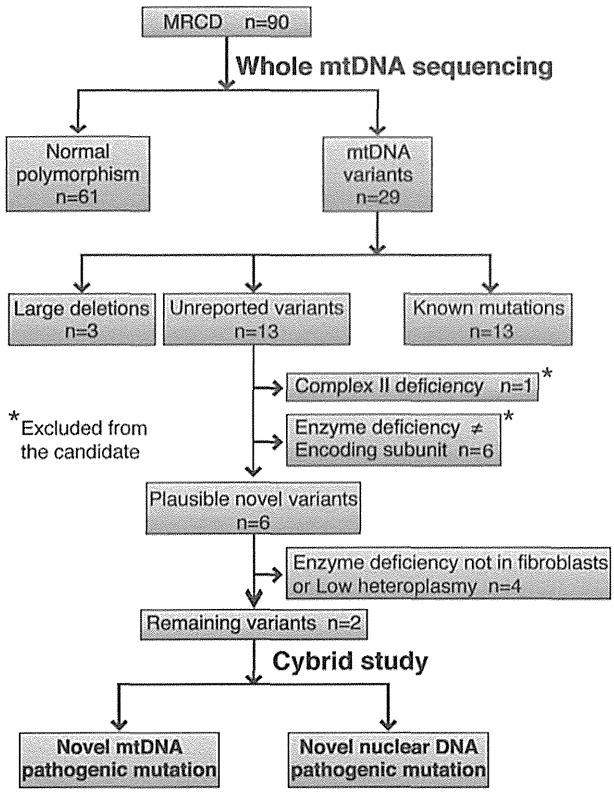

Figure 1. Flow diagram of study analysis. Ninety MRCD patients were analyzed in this study. Sixty-one patients had normal polymorphisms and 29 had mtDNA variants. Of these variants, 13 patients had MRCD causative mutations that had been previously described. We identified three novel large deletions and 13 unreported variants. Of the unreported variants, one patient with complex II deficiency was excluded because complex II is not encoded by mtDNA. Six patients were excluded because their enzyme deficiency pattern did not coincide with the variants found in mtDNA. Four patients were excluded because of the lack of fibroblast enzyme deficiency or low heteroplasmy. The remaining two cases were analyzed by cybrid study.

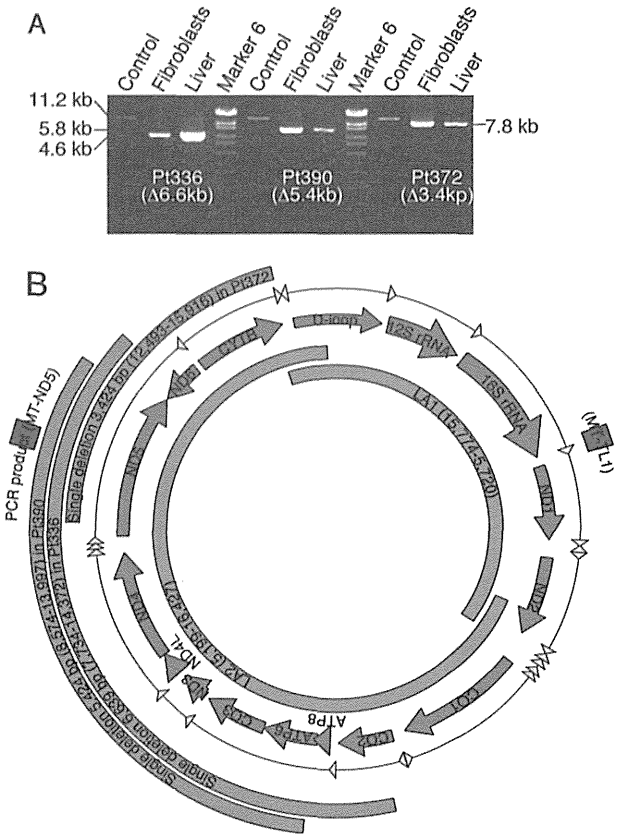

Figure 2. Identification of three large deletions. (A) Characterization of the three novel mtDNA deletions using agarose electrophoresis. First-round PCR products amplified from patient fibroblast and liver DNA clearly showed the presence of mtDNA deletions in Pt336, 390, and 372. Normal mtDNA from an MRCD patient was used as a positive control. (B) Positions of the novel mtDNA deletions are shown in blue. LA1 and LA2 amplification is shown in green. Two red squares represent real-time PCR amplicons MT-ND5 and MT-TL1.

analyzed for an mtDNA deletion. Second-round PCR was performed using fewer (25–26) PCR cycles to avoid untargeted DNA amplification. To identify the location of the deletion, we first compared the density of bands and screened the faint bands with agarose electrophoresis. The precise deletion boundaries were confirmed by sequencing analysis with primers used for second-round PCR that were close to the probable deletion region.

Results

Patient characteristics and their mtDNA mutations

A total of 90 patients (49 were men and 41 were women) with MRCD were subjected to whole mtDNA sequencing analysis (Table 1). Eighty-four subjects (93%) were non-consanguineous. Seventy-six subjects (84%) were aged 1 year or younger. We identified 13 previously reported mtDNA mutations, 13 unreported variants, and three novel deletions (Fig. 1). The remaining 61 subjects had normal polymorphisms in their mtDNA (Fig. 1).

Large mtDNA deletions were identified in three patients

Agarose gel electrophoresis of first-round PCR from fibroblast and liver mtDNA clearly showed the presence of mtDNA deletions in Pt336, 390, and 372 (Fig. 2A). The precise deletion sites were confirmed by sequencing analysis. The expected size of the first-round PCR LA2 product in wild-type mtDNA from an MRCD patient was 11.2 kb, which enabled us to estimate the deletion sizes

